SIV Rebound Kinetics Following TLR7-Agonist & Therapeutic Vaccine Administration

J.M. Gerold[1], C. Pasin[2], I. Balleli[2], S. Lim[3], C. Osuna[3], J.B. Whitney[3], D.H. Barouch[3], M. Prague[2], A.L. Hill[1]

[1]Program for Evolutionary Dynamics, Harvard University, Cambridge, USA. [2]Inria, Inserm U1219 BPH, SISTM team, University of Bordeaux, France; Vaccine Research institute, Créteil, Paris, France. [3]Beth Israel Deaconess Medical Center, Boston, MA, USA.

Abstract

Immunotherapy is a promising approach to prevent or control HIV rebound following cessation of antiretroviral therapy (ART). We conducted an in-depth characterization of viral load kinetics following ART interruption across multiple studies of TLR7-agonist treatment (innate immune stimulation) and therapeutic vaccination (viral vectors carrying gag-pol-env) in SIV-infected macaques. Our analysis uses a novel viral dynamics model that includes reactivation of latent infection and adaptive immune responses.

Study Design/Background

Treatment interruption studies in SIV-infected macaques provide insight into treatment mechanisms in a highly biologically relevant context. Two studies [1, 2] investigated the effects of immunotherapies administered during ART on viral rebound kinetics using similar treatment interruption frameworks. We performed a unified, model-driven analysis of these data in order to assess how each treatment impacted viral rebound. (**Fig. 1**).
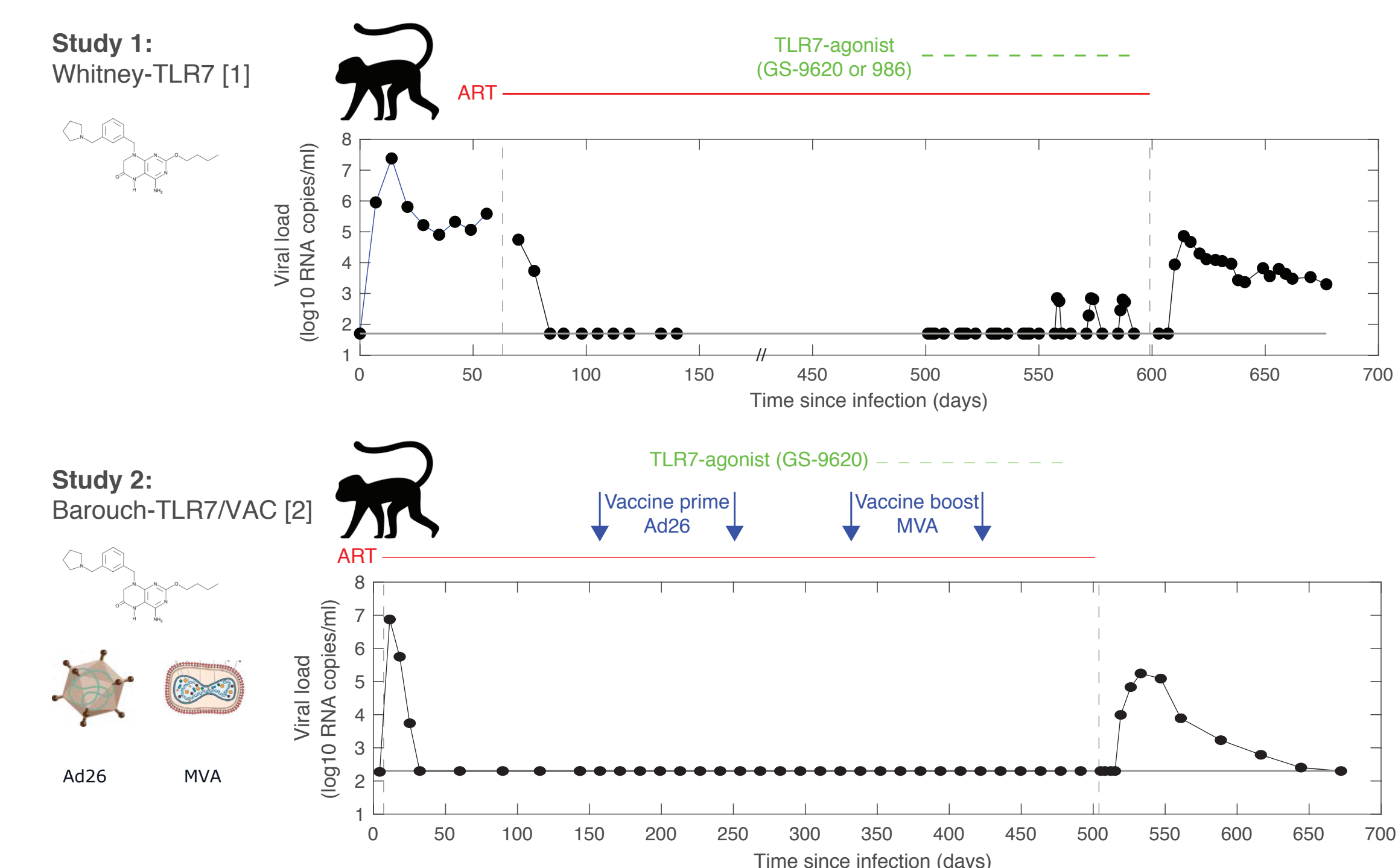

Fig. 1: Study Designs Overview.
– Study 1: Control, TLR7 Agonist GS-9620 or 986. 8 control and 13 treated macaques (21 total)
– Study 2: Control, TLR7 Agonist GS-9620, Vaccine, or Combination. 9 macaques in each group (36 total)

Model Schematic

Ordinary differential equation (ODE) models of viral infection underlie the understanding of HIV infection dynamics. However, standard models of viral rebound fail to capture the range of dynamic behaviors observed in these studies. **We developed an expanded model of viral dynamics to include an adaptive immune response and latency reactivation.**
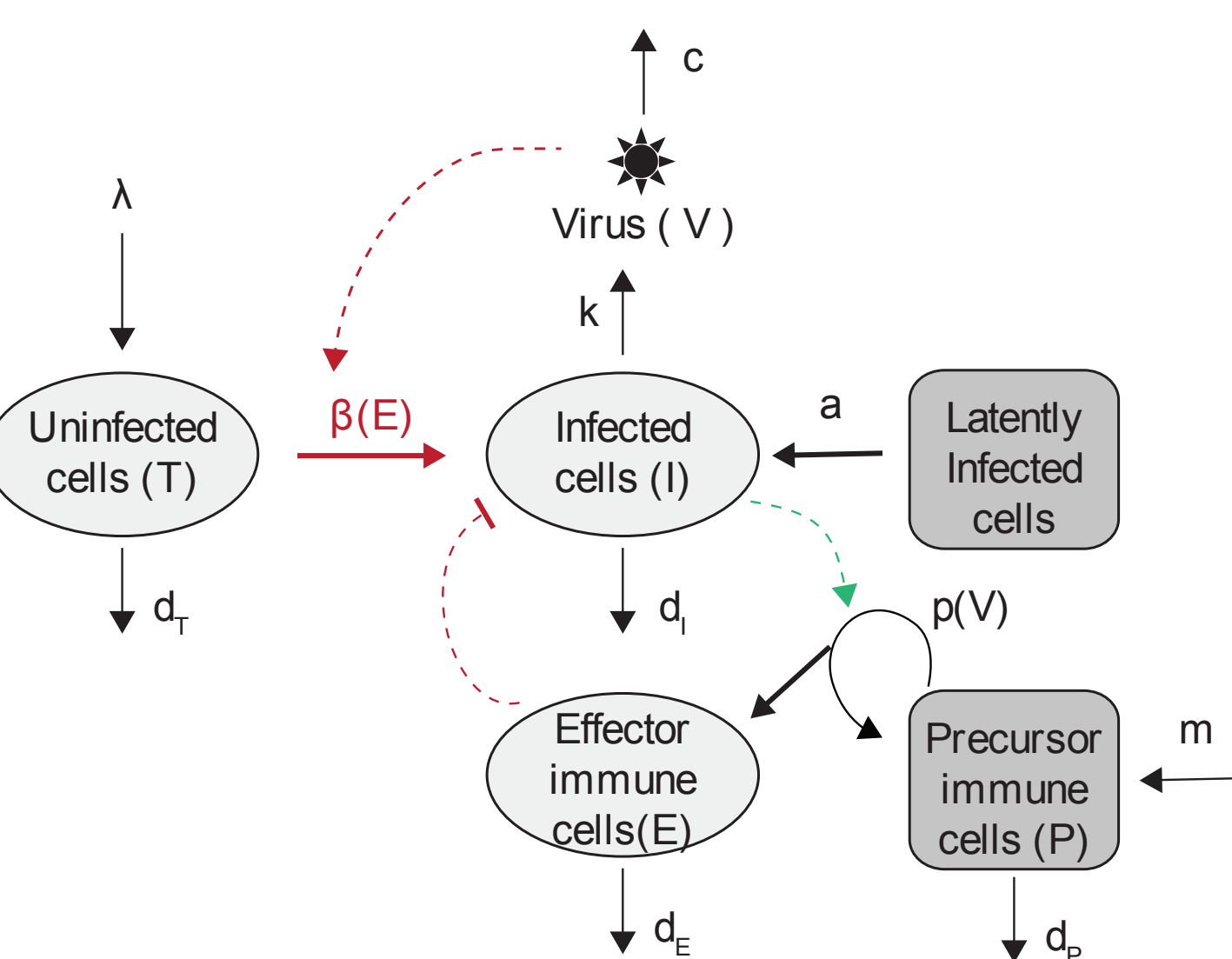

Fig. 2: Expanded model of viral dynamics. Virus v infects target cells T which become infected cells I and in turn produce virus. Immune precursor cells P interact with I and proliferate, giving rise to effector cells E, which inhibit infection. Finally, latently infected cells can restart infection by exiting from latency with rate a.

Model Equations

From our model schematic, we derived a system of ODEs which describes the dynamics of infection in the presence of an adaptive immune response. We do not model the establishment of the latent comparment, but instead treat the total rate of exit from the latent compartment as a parameter (a) in each subject.

$$\dot{T} = \lambda - \beta \mathbf{TV} - d_T \mathbf{T}$$
$$\dot{I} = a + \frac{\beta \mathbf{TV}}{1 + (\mathbf{E}/N_E)} - d_I \mathbf{I}$$
$$\dot{V} = k\mathbf{I} - c\mathbf{V}$$
$$\dot{P} = m + p(1-f)\mathbf{P}\frac{\mathbf{V}}{\mathbf{V} + N_p} - d_p\mathbf{P}$$
$$\dot{E} = pf\mathbf{P}\frac{\mathbf{V}}{\mathbf{V} + N_p} - d_E\mathbf{E}$$

$\mathbf{T}$, target cells.
$\mathbf{I}$, infected cells.
$\mathbf{V}$, free virus.
$\mathbf{P}$, immune precursors.
$\mathbf{E}$, immune effectors.

Model Behavior

We investigated how changes in different parameters affect viral rebound kinetics. Features of viral rebound are especially sensitive to changes in the viral infectivity β, the rate of latent cell reactivation a, the maximum rate of adaptive immune cell proliferation p, and the viral load at which half maximum proliferation occurs N_p.
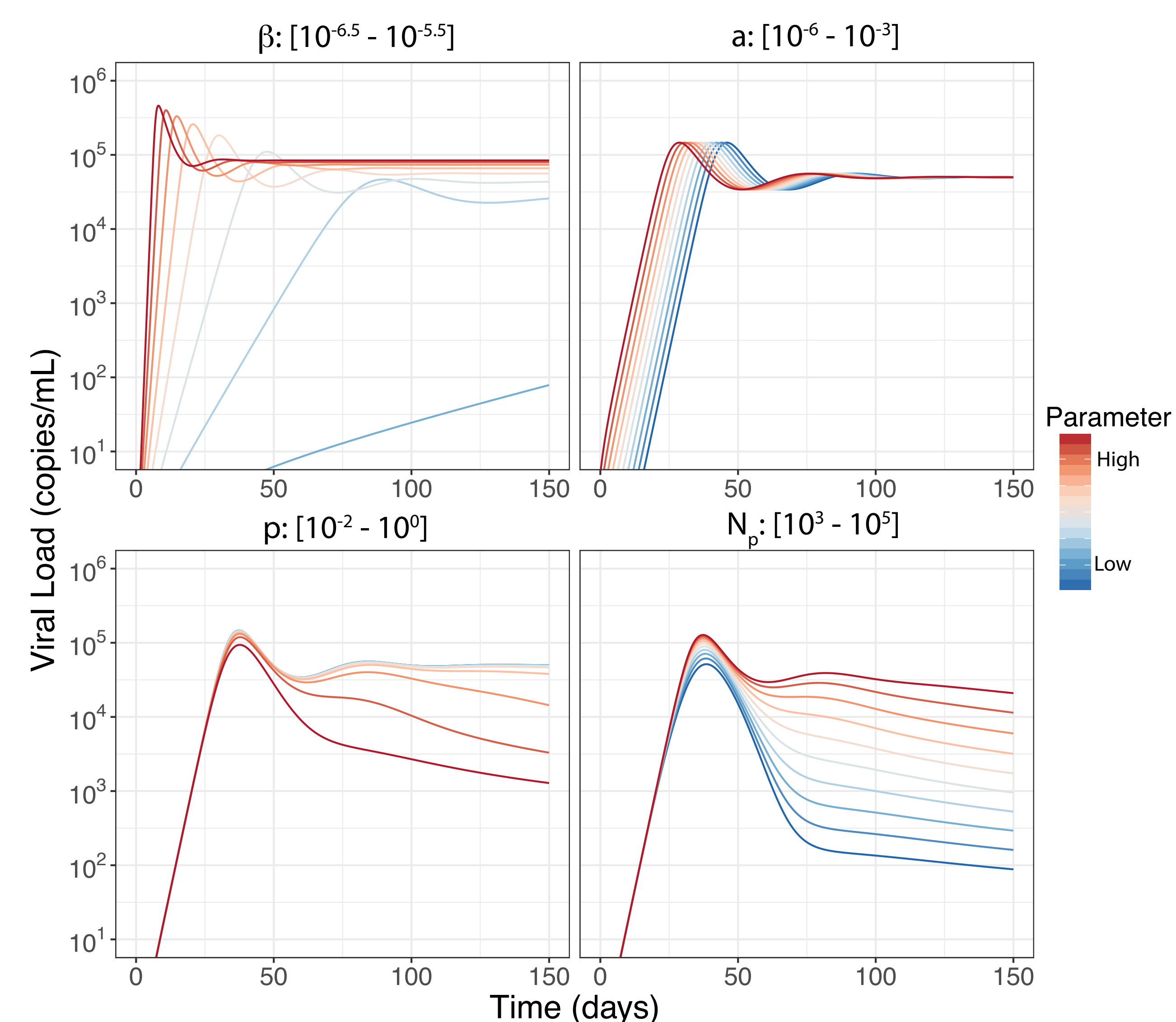

Fig. 4: Immune modulation alters infection dynamics. Each panel illustrates model viral load trajectories under variation in the indicated parameter. β (mL $copies^{-1}$ day^{-1}) controls the initial rate of viral growth and a ($cells$ day^{-1}) influences time to rebound. Additionally, when p (mL $copies^{-1}$ day^{-1}) is sufficiently high, an adaptive immune response drives viral load well below its peak. Combined with a large p parameter, N_p ($copies$ mL^{-1}) has a dramatic influence on the long-term behavior of the model.

References

[1] Lim et al., *Science Tran. Med.*, 2018. [2] Borducchi et al., *Nature*, 2017. [3] Bellu et al., *Comp. Meth. and Prog. Biomed.*, 2007. [4] Prague et al., *Comp. Meth. and Prog. Biomed.*, 2013. [5] Antony, France: Lixoft SAS, 2018. http://lixoft.com/products/monolix/

Parameter Reduction and Sensitivity Analysis

We reduced the number of parameters to be estimated with several methods. Fixed k and N_E lead to identifiable λ and m values. Further, we fixed c because it is practically non-identifiable due to the fast time-scale of the virus. Death rates of all immune cell populations and the fraction of proliferating effectors that return to long-lived memory were fixed at rates from the literature. For the model with remaining parameters $\beta, \lambda, a, m, p, N_p$ we performed comprehensive identifiability analysis with DAISY[3]: the model is locally identifiable and, with m fixed, globally identifiable. Finally, we also assessed the sensitivity of viral load to each parameter over time by evaluating $\frac{\partial V}{\partial \theta}\frac{\theta}{V}$.
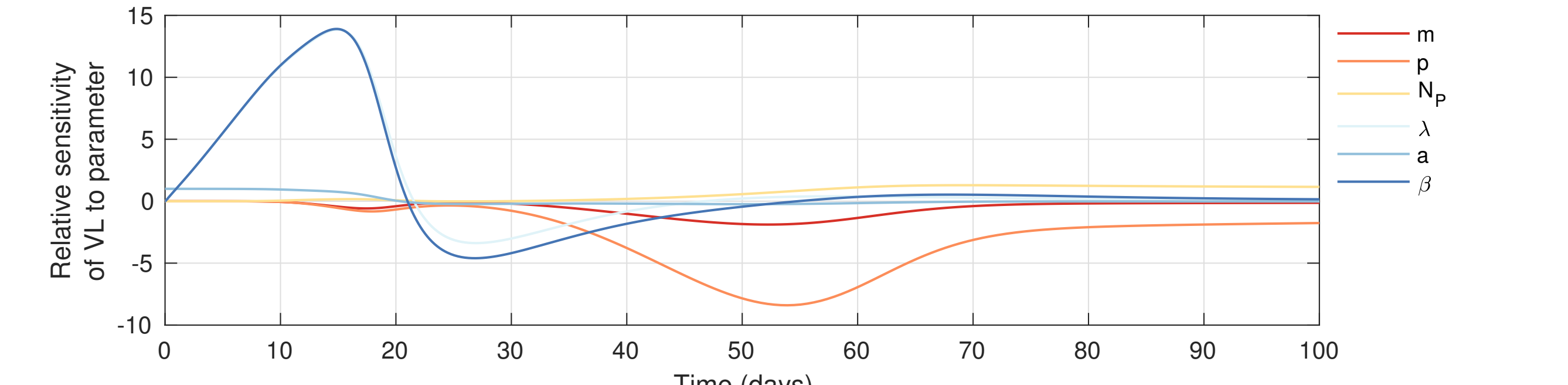
Fixed Parameter Values	
k	$5 \cdot 10^4$ $virus$ $cells^{-1}$ day^{-1}
c	23 day^{-1}
N_E	10^4 $cells$ mL^{-1}
d_T	0.05 day^{-1}
d_I	0.4 day^{-1}
d_p	0.001 day^{-1}
d_E	1 day^{-1}
f	0.9

Fig 5: Viral load sensitivity to model parameters. The viral load sensitivity over time to each free model parameter.

Individual Fits

Initially, we performed parameter fitting for each subject independently. In study 1, we restricted $p = 0$ to evaluate our hypothesis that treatment with the TLR7-agonist reduced the size of the latent reservoir. We observed that while several parameters varied between subjects, our estimates for a, the exit rate from the latent reservoir, was strongly associated with TLR7 treatment. In study 2, we allowed for an adaptive immune response ($p > 0$) and found that subjects treated with both TLR7-agonist and vaccine had the largest estimates of immune proliferation rate p and a suggestive effect of the vaccine on a. These observations motivated us to perform a more statistically powerful search for treatment effect [4].
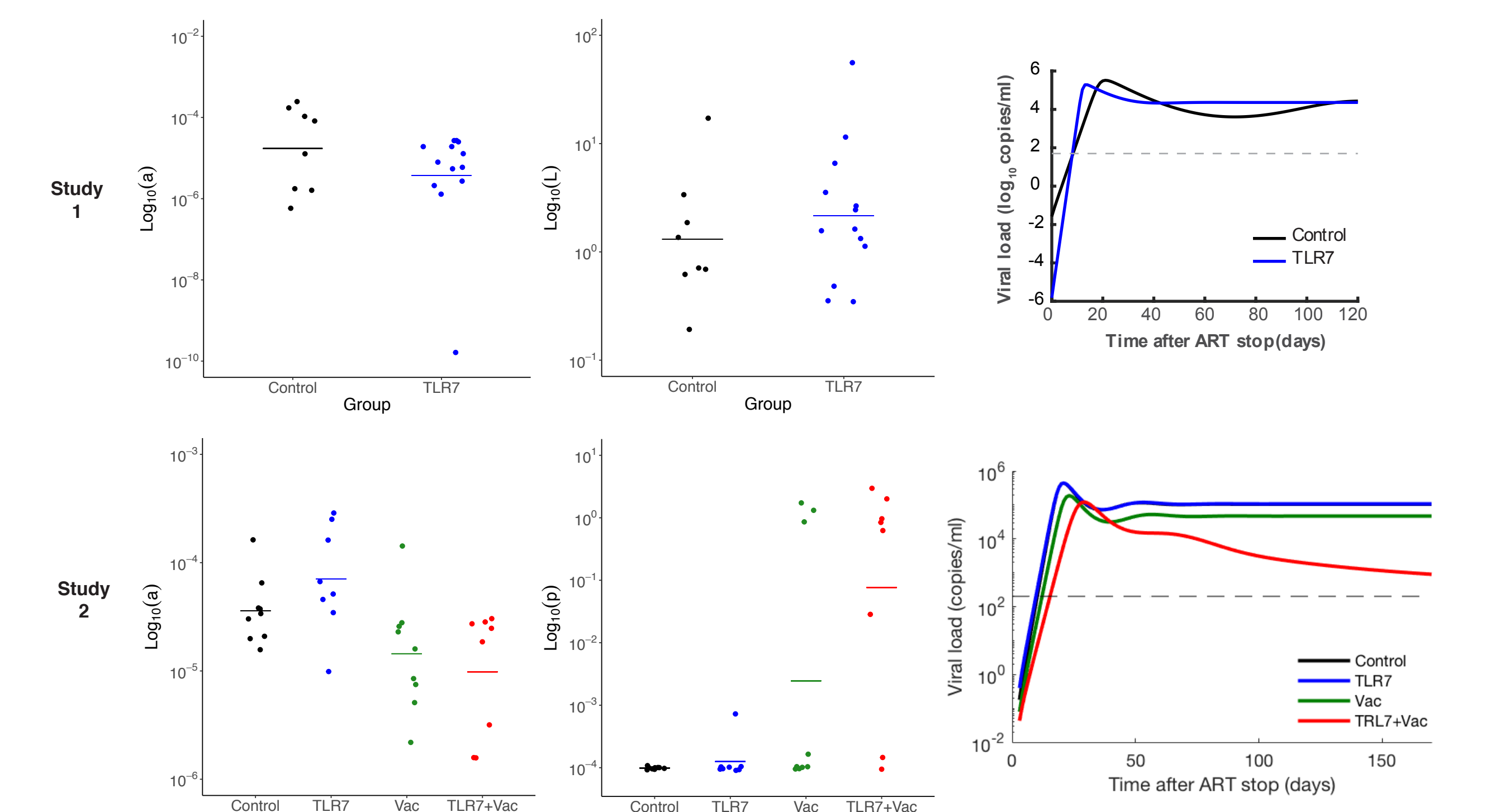

Fig. 6: Results of individual fits. Median *a posteriori* parameter values and group means for select parameters from studies 1 and 2. Right column shows the predicted viral load trajectory for each group for a hypothetical subject with mean parameter values. Our combined fitting approach (next panel) produced very similar predicted trajectories.

Population Fits Method

To evaluate differences between groups in a statistically rigorous way, we used a mixed-effects modeling framework implemented in Monolix[5]. After fixing a value for m by profile-likelihood, we allowed all other parameters $\beta, \lambda, a, p, N_p$ to have random effects. We removed random effects in an iterative manner if found to be non-significant. We also considered group-level effects of immunotherapy (TLR7, Vac) and study (early vs late ART) on each parameter. We used an iterative, forward selection approach to add effects that improved model likelihood, but we removed effects if they were found not significant at any later stage.

Population Fits Results

Our best-fit model suggested that TLR7-agonist treatment resulted in a 30-fold reduction the LR ($\downarrow a$) and a 5-fold increase in immune avidity ($\downarrow N_p$). Vaccination resulted in a 15-fold LR reduction and a 50-fold boost in immune avidity. Finally, delayed ART-start was associated with 3-fold increase in maximum immune proliferation ($\uparrow p$).
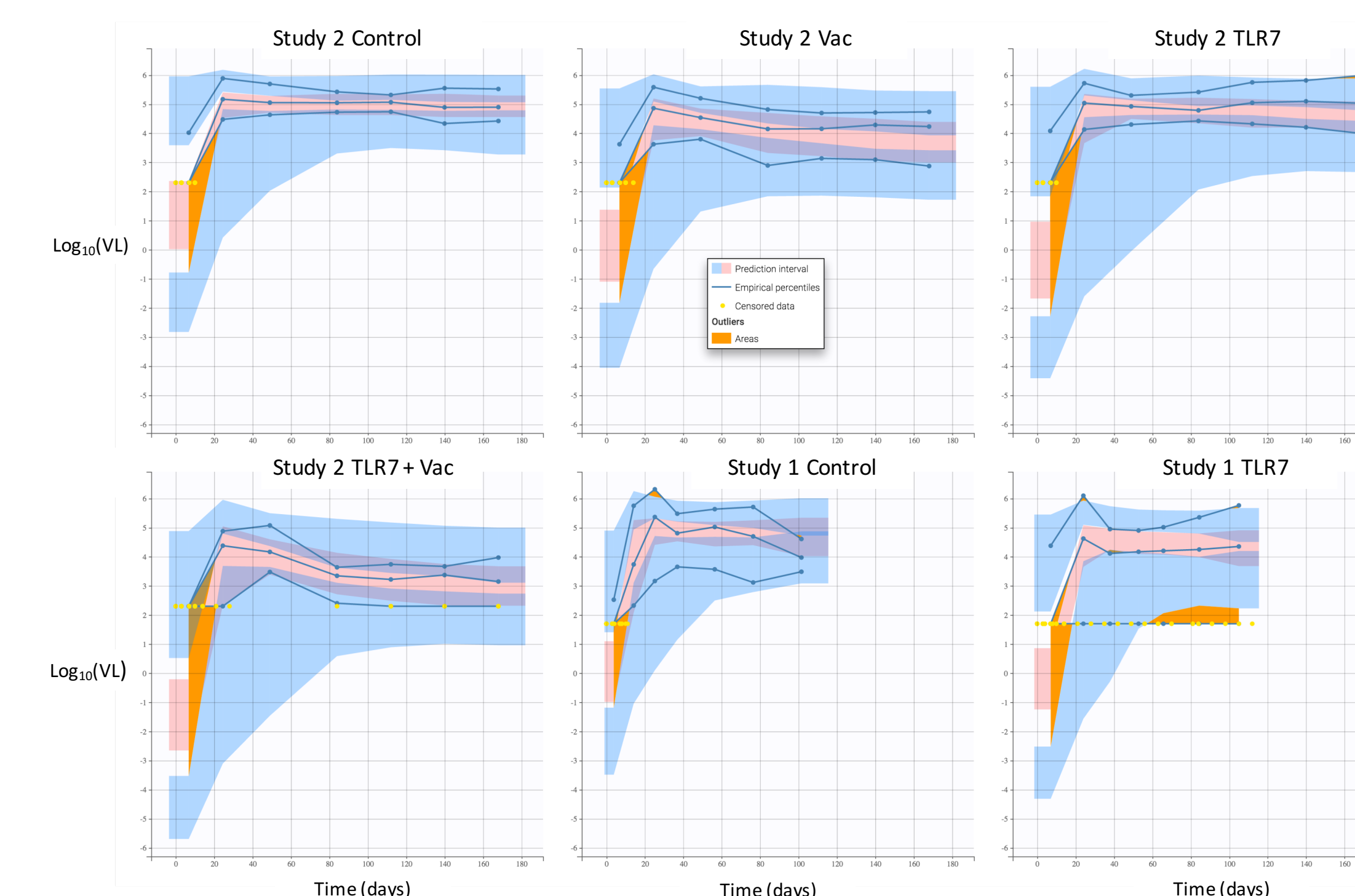

Fig 7: Posterior predictive check for model fit. Lines show empirical data variation (10th percentile, median, and 90th percentile) and shaded regions indicate the distribution of predicted data after fitting. Orange highlights regions of poor overlap between data and model predictions. Overall, simulated trajectories in each group show good agreement with observed data, in particular for median trajectories.

Blip Size Estimation

In Study 1, viral blipping was observed during TLR7-agonist dosed animals despite the presence of ART, suggesting latency reactivation. We used an augmented model (Fig 8a) to estimate how many cells would have been required to exit from latency to produce the observed blip sizes. **The data are consistent with a significant proportion of intact virus (i.e. 1% of all SIV-DNA+ cells) being reactivated over the treatment course.** Further, 2/13 animals did not rebound even after CD8 depletion, supporting a reduction of latent virus leading to sterilizing cure.
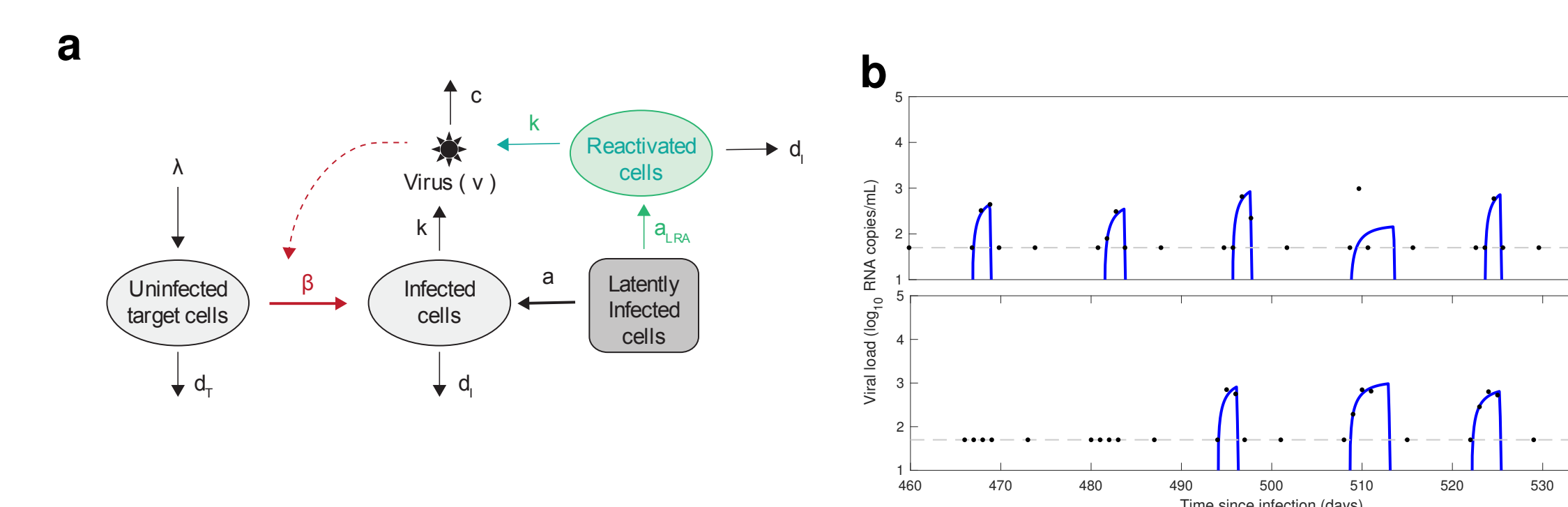

Fig. 8: Virus production through latent cell reactivation. Schematic of augmented model to include latency reactivation and absence of new infection (assuming fully-effective ART). We assume that each TLR7-agonist dose causes reactivation of latent cells with rate a_{LRA} for a time period t_{LRA}. Drug-reactivated cells are assumed to produce virus and die the same rate as naturally-reactivated cells. We fit a_{LRA} and t_{LRA} for each dose in each patient from the blip time course, and used this to calculate total latent cells reactivated.

Conclusions

We found that TLR7-agonist administered during chronic infection can lead to some reductions in the functional latent reservoir in most animals and complete clearance in others, while the post-treatment control obtained with TLR7+therapeutic vaccination is also supported by immunologic stimulation.